Denoising and Compressing Color Images Using New Wavelet Efficiency

Hanaa Mahdi Habeb[1], Zainab Galib Salman Alrashid[2], Saad Ismael Ibrahim[3], Asma A. Abdulrahman[4], Hassan Mohamed Muhi-Aldeen[5,*]

[1]Department of computer science, University of Technology, 52 Alsena str., Baghdad, 10053, Iraq

[2]Aliraqia University, 22Aladamia, Baghdad, Iraq

[3]College of Media -Unit of Rehabilitation Employment and Fallow Up, Al-Iraqia University, Iraq

[4]Department of Applied Sciences, University of Technology, 52 Alsena str., Baghdad, 10053, Iraq

[5]Department of Computer Engineering, Aliraqia University, 22Sabaabkar, Adamia, Baghdad, Iraq

Emails: hanaa.m.habeb@uotechnology.edu.iq; zainab_alrashid@aliraqia.edu.iq; saad.i.ibrahim@aliraqia.edu.iq; asma.a.abdulrahman@uotechnology.edu.iq; muhialdeen.hassan@aliraqia.edu.iq

Abstract

Compressing color images (such as JPEG 2000) with wavelet transforms that are used in image parsing into approximate and detailed coefficients in the Multi Resolution Analyses (MRA) stage, such as Symlet 2, Coiflet 2, and Daubechies 2. The rapid development that occurs in modern life and the development of technology and artificial intelligence has increased the need to find an advanced and fast technology in image transfer, which requires reducing the space used by very large image data through the compression process that images need during transfer and transmission. Therefore, the need to accomplish this work has been necessitated by finding a new method and purely mathematical methods with equations and transformations that will be performed on Hermite polynomials to obtain the discrete Hermite wavelets (DHWT) to meet the great challenge in the field of images due to the mathematical properties that characterize these waves to be ready to perform the image analysis process known in the field of images (MRA), which is summarized in entering the color image to analyze the color image into two types of coefficients, which are detail coefficients and convergence coefficients due to the high level and low level, respectively, to divide the image into four blocks, which are Low Low, High Low, Low High and High High to then remove the noise and then compress, A suitable algorithm was created in MATLAB to read the program for this tool as in common waves (Symlet 2, Coiflet 2, and Daubechies 2) to obtain good results with new wavelet. The results obtained and through comparisons with basic wavelet work such as Haar and Daubechies etc. to obtain the values of the most important image quality parameters and the experiment was carried out on a sample of JPEG 2000 The tables in this work show the results that will be obtained that prove the efficiency of the proposed model after calculating the image quality parameters Mean Square Error (MSE), Peak Signal of Noise Ratio (PSNR), Bit Per Pixel (BPP) and Compassion Ratio (CR).

Keywords: JPEG 2000; Color image; Wavelet; New algorithm; Multi Resolution Analyses

1. Introduction

Image analysis and compression procedures could be made simpler by developing a wavelet transformation. DWT [1] benefited greatly from this wavelet processing and became more popular than its predecessors. This is similar to DCT [2], but DWT has the continuity property [4], which makes it consume less energy [5], however, DCT generates better compressed images than DWT. If the resultant image information is preserved, even in the event of

DOI: https://doi.org/10.54216/JCIM.160208
Received: January 30, 2025 Revised: March 23, 2025 Accepted: April 11, 2025

a loss [6], it will remain undetectable [7]. When comparing the non-losing compression [8] with the losing compression [9], then see that the latter has a minor, imperceptible difference, while the former has high compressed ratios. Previous transformations used in image processing to convert pixels to frequency coefficients [10], resulting in the loss of image data. To get extremely accurate images from the analysis of the color image, either smooth images or wavelets are used [11]. New results will be obtained using the limits [12]. The large numbers of images and the data that these images carry require transformations that convert the image into binary matrices through the computer to be the machine that stores this data and the need to compress this data [13-16]. Which requires sufficient storage space [17]. Achieving the quantitative measurement procedure to obtain the pressure [18], [19]. For wireless sensor networks, duplicating data that requires high frequencies can be challenging [20]. Image compression technology provides a solution to these problems. [21]. Use arrays (NMF) to obtain a general understanding of the data's dimensions, In the medical field, compression methods have been used, including Singular Value Decomposition (SVD) to send images [22]. send images using it. In the medical domain, image compression seeks to reduce file size without compromising the quality of the original image. Digital images are available [23]. The industry standard for storing patient data in medical imaging files is Digital images Compression Of Medical (DICOM). Hoffman lossless compression is used to compress the data instead of DICOM [24].

Wavelets and the EZW algorithm were used to compress the color image to achieve superior compression results because of Wavelets provide a relative lossless compression value in the original image data. Using the discrete Hermite wavelet transform (DHWT), a color image was compressed in this work [27]. The wavelets were examined and divided into approximation and detailed coefficients once they were supplied to the MATLAB code. To determine the correct filter, validate its mathematical components, and test it using an operation and a matrix, Multi-Resolution Analyses (MRA) [25] were used. Decomposition with rows, reconstruction using the filter's inverse [26], and modification of the matrix's columns were the methods used to obtain the original matrix. The new filter was integrated into the MATLAB program using a new technique, enabling the wavelet to be used with the other common wavelets in the program, such as Symlet 2, Coiflet 2, and Daubecheis2. Works in which images were processed by creating new wavelets from polynomials of Laker, Chebyshev, Legendre, etc. These new tools in the field of images are also used in artificial intelligence [27-30].

In this work, a good model will be used to produce new Hermit waveforms that can be used in good image processing and obtain the most important results that have been compared with previous models. Tables (2) and (3) prove the efficiency of the proposed theory.

2. Materials and methods

2. 1. Proposed method

The proposed transforms in this study are applied to the image shown in Fig. 1 during the Multi-Resolution Analysis (MRA) stage, in order to generate discrete Hermite wavelets derived from Hermite polynomials. These wavelets are constructed based on the mother function defined in Equation (1).

$$h_{a,b}(x) = |a|^{\frac{-1}{2}} h\left[\frac{x-b}{a}\right] a, b \in R, a \neq 0 \qquad (1)$$

With the transform $a = 2^{-k}$, $b = \big(a(2n-1)\big), x = a(2a^{-1}t)$, and DHWT $h_{n,m}(t) = h(k,n,m,t)$ in equation (12) in [0,1].

$$h_{n,m}(t) = \begin{cases} 2^{\frac{k}{2}} H_m^*\big(2^{k+1}t - 2n + 1\big) t \in \left[\frac{n-1}{2^k}, \frac{n}{2^k}\right] \\ 0 \qquad \text{otherwise} \end{cases} \qquad (2)$$

Where $H_m^* = \frac{1}{2^m m!\sqrt{\pi}} H_m \qquad m = 0,1,2,\dots,M-1 n = 0,1,2,\dots,2^k$

The approxemate function in [0,1]

$$f(t) = \sum_{n=1}^{\infty} \sum_{m=0}^{\infty} c_{n,m} h_{n,m}(t) \qquad (3)$$

where $C_{n,m} = \big(f(t), h_{n,m}(t)\big) = \int_0^1 w_n(t) h_{n,m}(t)\, f(t) dt$ in which $\langle .,. \rangle$denoted inner product in $L^2_{w_n}[0,1]$.

DOI: https://doi.org/10.54216/JCIM.160208
Received: January 30, 2025 Revised: March 23, 2025 Accepted: April 11, 2025

A certain limit is taken from the terms in the equation (4)

$$(ft) \cong f_{2^k,M-1} \sum_{n=1}^{2^k} \sum_{m=0}^{M-1} C_{n,m} h_{n,m}(t) = C^T h(t) \quad (4)$$

where F and $h(t)$ are $2^k M \times 1$ matrices given by:

$$h(t) = \left[h_{1,0}(t), h_{1,1}(t), \dots, h_{1,M-1}(t), h_{2,0}(t), \dots, h_{2,M-1}(t), \dots, h_{2^k,0}(t), \dots, h_{2^k,M-1}(t)\right]^T,$$

$$C = \left[C_{1,0}, C_{1,1}, \dots, C_{1,M-1}, C_{2,0}, \dots, C_{2,M-1}, \dots, C_{2^k,0}, \dots, C_{2^k,M-1}\right]^T \quad (5)$$

The Hermite wavelet transform, with $\in R$, with time t can be defined the coefficients

$$A_{a,b} = \int_R f(t) h_{a,b}(t) dt \; a \in R^+, b \in R \quad (6)$$

used scaling function in orthogonal with wavelet function h can be get the two basic wavelets are called Hermite wavelets in equation (7)

$$\begin{cases} h_{n,m}(t) = 2^{\frac{k}{2}} h\left(2^{k+1} t - n + 1\right) \\ \omega_{n,m}(t) = 2^{\frac{k}{2}} \omega\left(2^{k+1} t - n + 1\right) \end{cases} \quad (7)$$

$for (n, m) \in Z^2$

With coefficients in (8) and (9)

$$\delta_{n,m} = \int_R S(t) h_{n,m}(t) dt \quad (8)$$

$$\eta_{n,m} = \int_R S(t) \omega_{n,m}(t) dt \quad (9)$$

The reconstructed the signal

$$S(t) = \sum_{n \in Z} \sum_{m \in Z} h_{n,m}(t) \delta_{n,m} \quad (10)$$

The concept of Multi Resolution Analysis (MRA)

with $f(t) \in V_n \Leftrightarrow f(2t) \in V_{n-1}$, be defined (11)

$$V_0 = \left\{ f \in L^2(R) \middle| f(t) = \sum_{n \in Z} A_{n,m} \omega\left(2^{k+1} t - 2n + 1\right) \in l^2(Z) \right. \quad (11)$$

The wavelet spaces denoted by$\{W_n\}_{n \in Z}$, the space $W_n \perp V_n$ in $V_{n-1} = V_n \oplus W_n, n \in Z$, $\{\omega_{n,m}\}(n, m) \in Z^2$is generated $\{V_n\}_{n \in Z}$ and $\{h_{n,m}\}(n, m) \in Z^2$ is generated $\{W_n\}_{n \in Z}$, the coefficient $\delta_{n,m}$ is the orthogonal projection of S on $\{W_n\}_{n \in Z}$.

The approximation coefficients of DHWT is

$$\eta_{n,m} = \int_R S(t) \omega_{n,m}(t) \, dt \quad (12)$$

where $A_n(t) = \sum_{m \in Z} \eta_{n,m} \omega_{n,m}(t)$ (13)

The detail coefficients of DHWT is

$$\delta_{n,m} = \int_R S(t) h_{n,m}(t) \, dt, \quad (14)$$

where $D_n(t) = \sum_{m \in Z} \delta_{n,m} h_{n,m}(t)$ (15)

DHWT is applied on a 4×4sub-image for more illustration**.** The coefficients of DHWT obtained above are used where the filter extracted is

$$(2 \times 2)F = \frac{1}{\sqrt{\pi}} \begin{bmatrix} 1 & -1 \\ 1 & 1 \end{bmatrix} \quad (16)$$

Image analysis in the MRA phase using DHWT is illustrated in Fig.1.

DOI: https://doi.org/10.54216/JCIM.160208
Received: January 30, 2025 Revised: March 23, 2025 Accepted: April 11, 2025

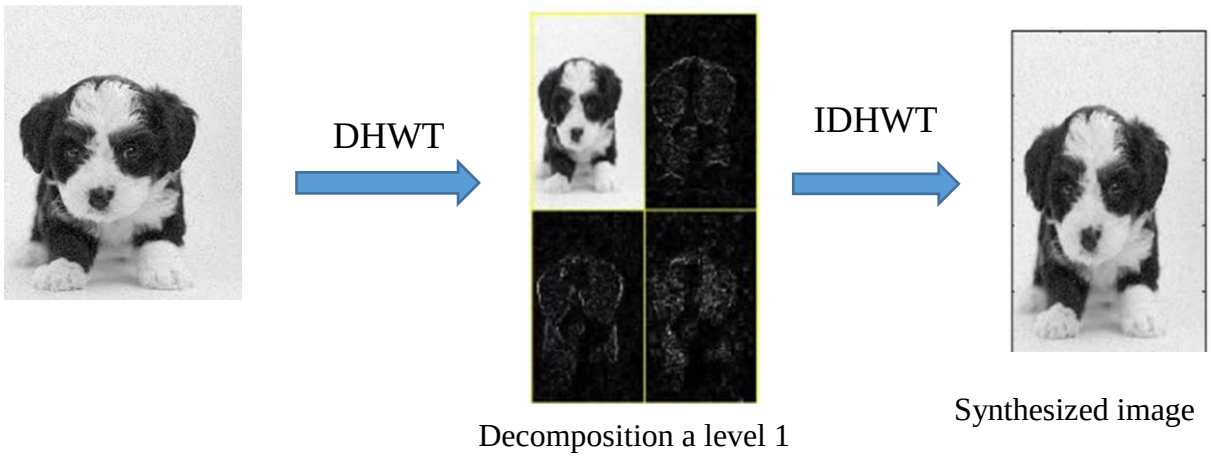

Figure 1. Analysis image with DHWT in MRA

2.1. Proposed Model Algorithm in Color Image Compression

Image compression algorithm steps with the proposed model, enter color image

Step 1: Using the new wavelets proposed in this work after inserting them into MATLAB.

Step 2: wavelets are divided into low pass filter and high pass filter so that th coefficients are divided into approximate coefficient and details coefficient

Step 3: The image analysis stage into four parts LL, LH, HL, HH The first represents the approach coefficients, while the remaining parts represent the detail coefficients; each part has a size 16x16.

Step 5: Taking the quadrant LL that represents approach coefficients to denoise from the resulting image.

Step 6: The image is compressed in several stages as in the table that shows the compression stages.

Step 7: Taking the inverse of the wavelet proposed in this work restores the processed image without losing input image information.

Figure 2 illustrates the stages involved in the color image compression process using the proposed system.

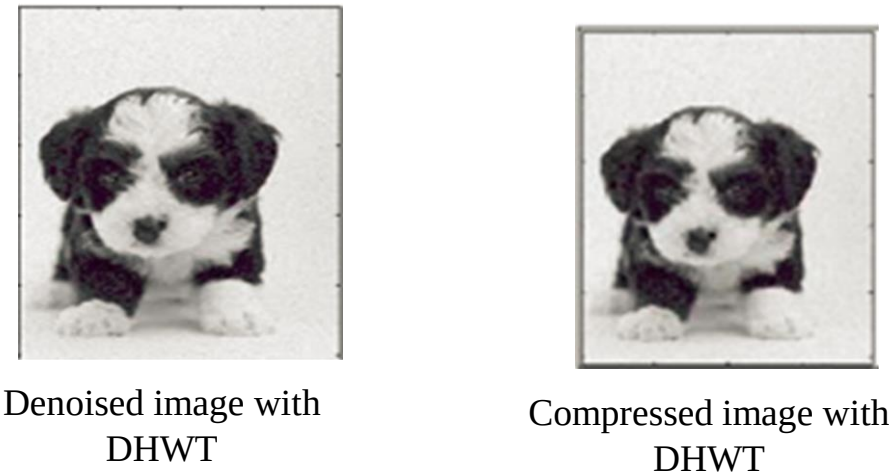

Figure 2. Denoised and Compressed image with DHWT

DOI: https://doi.org/10.54216/JCIM.160208
Received: January 30, 2025 Revised: March 23, 2025 Accepted: April 11, 2025

3. Results and Discussion

In this section, the results are presented, discussed, and compared with other waveforms such as Daubechies 2, Symlet 2, and Coiflet 2 to illustrate the superior performance of the proposed waveforms. The proposed waveforms achieved the best results in MSE and PSNR. At high levels of decomposition, specifically at level 8, an ideal PSNR value of 46.99 was achieved, which is favorable compared to other waveforms. Additionally, the compression ratio (CR) reached 46.17%, indicating no effective loss of quality.

Tables 1 and 2 contain comparison results for the basic wavelets with the proposed wavelets at level 8 that demonstrate the quality achieved compared to those wavelets. Using MATLAB and at the prompt of Wavelet Toolbox, DHWT was added to the mentioned program to apply the proposed wavelets to the color image

Color image compression is improved with the proposed wavelet and the results are obtained from it

1- MSE (Maximum Signal-to-Noise Ratio): Increased from 7.712 dB to 46.99 dB, reflecting superior image quality after compression.

2- In return for the decrease in MSE error, the PSNR value increased from 7.712 dB to 46.99 dB, indicating improved compressed image quality.

3- The image was improved with BPP value, where the value was improved from 0.0072 to 11.081, achieving a balance for image quality.

4- The CR value achieved 46.17%, indicating that important information of the image was preserved while reducing the space occupied by the data

In the MRA stage, the approximate coefficients LL and details LH, HL and HH are separated with a threshold that is the reason for the critical features to remain. This means that the proposed wavelet is successful and the image is restored without loss with the inverse wavelet DHWT. In calculations and trade-offs, the proposed wavelet DHWT takes time to reach the optimal solution because it is achieved at level 8. This indicates that DHWT is suitable for applications where quality is prioritized over speed, such as medical applications and archive storage.

The obtained results with PSNR and MSE values are suitable for applications to DICOM files for medical applications and wireless sensors to be lossless compression for researcher accessibility via the Wavelet Toolbox in MATLAB. A strength of this technique in this work is the mathematical approach used to derive the DHWT from Hermite polynomials and its orthogonality capability, which enhances the obtained compression efficiency. The proposed method demonstrates the ability to adaptively adjust thresholds at each level of the decomposition process, allowing for more precise control over image compression quality. However, the computational complexity associated with the DHWT framework introduces certain limitations, particularly in terms of processing time during multi-level decomposition. Despite these challenges, the method underscores the significance of DHWT in enhancing the overall compression workflow, especially in applications that demand high accuracy and data fidelity.

Table 1: Represents the compression stages of the input image with the new Wavelets DHWT

Loop	CI	MSE	PSNR	BPP	CR
1		11010	7.712	0.0072	0.03%
2		3664	12.5	0.0076	0.03%
3		3094	13.23	0.0079	0.03%
4		3094	13.23	0.0079	0.03%

DOI: https://doi.org/10.54216/JCIM.160208
Received: January 30, 2025 Revised: March 23, 2025 Accepted: April 11, 2025

5		2008	14.98	0.0113	0.05%
6		1669	15.91	0.015	0.07%
7		1030	18	0.046	0.19%
8		619.3	20.21	0.110	0.46%
9		278.4	23.69	0.319	1.33%
10		124.4	27.18	0.633	2.64%
11		53.76	30.83	1.1752	4.90%
12		21.41	34.82	2.074	8.64%
13		8.404	38.89	3.388	14.12%
14		3.443	42.76	5.343	22.27%
15		1.758	45.68	7.941	33.09%
16		1.302	46.99	11.081	46.17%
17		1.302	46.06	11.081	46.17%
18		1.302	46.99	11.081	46.17%

DOI: https://doi.org/10.54216/JCIM.160208
Received: January 30, 2025 Revised: March 23, 2025 Accepted: April 11, 2025

DOI: https://doi.org/10.54216/JCIM.160208
Received: January 30, 2025 Revised: March 23, 2025 Accepted: April 11, 2025

Table 2: It shows the most important readings that prove the efficiency of the proposed work with other techniques

DHWT				
point	**MSE**	**PSNR**	**BPP**	**CR**
1	7.050	39.050	25.102	4726%
2	4.7201	40.45	17.676	72.65%
3	3.222	41.30	10.102	45.26%
4	3.200	41.50	7.344	26.60%
5	3.100	42.44	8.640	30.38%
6	2.22	43.30	9.720	35.65%
7	1.84	44.21	11.091	45.17%
8	1.405	45.99	11.081	46.17%
SYM 2				
point	**MSE**	**PSNR**	**BPP**	**CR**
1	9.850	38.65	24.2	45.01%
2	6.922	40.44	16.99	60.80%
3	5.924	41.25	10.734	46.62%
4	5.2	41.82	6.2	30.8%
5	5.3	41.75	6.43	28.9%
6	4.2	41.70	6.5	25.7%
7	4.5	41.7	6.4	27.4%
8	2.8	42.85	12.0	55.8%
COIF 2				
point	**MSE**	**PSNR**	**BPP**	**CR**
1	9.9	39.1	25.0	99.0%
2	6.488	41.02	15.320	65.00%
3	8.55	39.8	8.5	33.44%
4	3.19	41.`1	7.7	25.1%

DOI: https://doi.org/10.54216/JCIM.160208
Received: January 30, 2025 Revised: March 23, 2025 Accepted: April 11, 2025

5	4.10	44.1	8.5	26.1%
6	4.40	43.1	9.4	22.9%
7	4.60	41.1	8.4	24.8%
8	2.54	40.01	11.5	54.4%
db2				
point	**MSE**	**PSNR**	**BPP**	**CR**
1	11.0	36.1	21.5	92.8
2	5.592	39.41	15.991	71.8%
3	9.15	38.33	9.1	33.0%
4	4.15	**41.55**	**8.3**	**31.6%**
5	4.35	**41.55**	**7.2**	**30.7%**
6	4.48	**41.42**	**7.3**	**30.4%**
7	4.38	**41.12**	**7.5**	**32.4%**
8	2.17	**4.27**	**8.9**	**45.4%**

4. Conclusion

In this study, the Discrete Hermite Wavelet Transform (DHWT), which is derived from Hermite polynomials, is employed to compress input images with a high degree of precision. Unlike traditional wavelet techniques, DHWT offers a unique mathematical structure based on orthogonal polynomials, enabling more adaptive and localized signal representation. The process begins with Multi-Resolution Analysis (MRA), where the input image is decomposed into hierarchical sub-bands—specifically approximation and detail coefficients—using a newly designed filter bank tailored for Hermite-based wavelets. This decomposition captures both low-frequency structural information and high-frequency textural features, making it highly efficient for compressing images without sacrificing critical details. After the decomposition stage, the image can be accurately reconstructed using the Inverse Discrete Hermite Wavelet Transform (IDHWT), which reverses the transformation and restores the original structure. The proposed system demonstrates superior performance in preserving image fidelity while significantly reducing data redundancy. This is particularly beneficial in fields like medical imaging, where even slight distortions or data loss can affect diagnostic accuracy. The DHWT-based method outperforms conventional wavelet techniques by maintaining a better balance between compression ratio and image quality. Quantitative assessments, such as Peak Signal-to-Noise Ratio (PSNR) and Structural Similarity Index (SSIM), support the method's effectiveness in maintaining visual and structural integrity in compressed medical images. Looking ahead, the integration of the proposed DHWT-based compression system with deep learning frameworks presents a promising research direction. Combining the high-efficiency compression capabilities of DHWT with the adaptive learning power of deep neural networks could lead to advanced hybrid systems capable of automated feature extraction, classification, and intelligent compression tailored to specific imaging tasks. Such integration may enhance performance in various applications, including medical diagnostics, biometric recognition, remote sensing, and image-guided systems. Future work will focus on exploring convolutional neural networks (CNNs), autoencoders, and transformer-based models that can work synergistically with DHWT to further improve performance, scalability, and real-time applicability.

Funding: "This research received no external funding"

Conflicts of Interest: "The authors declare no conflict of interest."

DOI: https://doi.org/10.54216/JCIM.160208
Received: January 30, 2025 Revised: March 23, 2025 Accepted: April 11, 2025

References

[1] M. I. Razzak, S. Naz, and A. Zaib, "Deep learning for medical image processing: Overview, challenges and the future," Classification in BioApps, 2018, pp. 323–350.

[2] R. Li and W. Zhang, "Deep learning based imaging data completion for improved brain disease diagnosis," International Conference on Medical Image Computing and Computer-Assisted Intervention, 2014, pp. 305–312.

[3] Y. A. A. S. Aldeen, M. Salleh, and M. A. Razzaque, "State of the art survey on security issue in cloud computing architectures, approaches and methods," Journal of Theoretical and Applied Information Technology, vol. 75, no. 1, pp. 53-61, 2015.

[4] E. Colleoni, S. Moccia, and X. Du, "Deep learning based robotic tool detection and articulation estimation with spatio-temporal layers," IEEE Robotics and Automation Letters, vol. 4, no. 3, pp. 2714–2721, 2019.

[5] D. P. Yadav, A. Sharma, M. Singh, and A. Goyal, "Feature Extraction Based Machine Learning for Human Burn Diagnosis From Burn Images," IEEE Journal of Translational Engineering in Health and Medicine, vol. 7, pp. 1-7, 2019.

[6] M. Ahmed and F. Khalifa, "A deep learning based system for accurate diagnosis of brain tumors using T1-w MRI," Indonesian Journal of Electrical Engineering and Computer Science, vol. 28, no. 2, pp. 1192–1202, 2022, doi: 10.11591/ijeecs.v28.i2.pp1192-1202.

[7] A. G. Diab and N. Fayez, "Accurate skin cancer diagnosis based on convolutional neural networks," Indonesian Journal of Electrical Engineering and Computer Science, vol. 25, no. 3, pp. 1429–1441, 2022, doi: 10.11591/ijeecs.v25.i3.pp1429-1441.

[8] A. Ishwarya, R. Janani, A. Nishanthi, and P. Kumar, "Kidney stone classification using Deep Neural Networks and facilitating diagnosis using IoT," International Research Journal of Engineering and Technology (IRJET), vol. 6, no. 3, pp. 8178, Mar. 2019.

[9] A. M. Al-Khafagy, S. R. Hashim, and R. A. Enad, "A unique deep-learning-based model with chest X-ray image for diagnosing COVID-19," Indonesian Journal of Electrical Engineering and Computer Science, vol. 28, no. 2, pp. 1147–1154, 2022, doi: 10.11591/ijeecs.v28.i2.pp1147-1154.

[10] S. Patel, B. Talati, S. Shah, and B. Y. Panchal, "Bone fracture classification using modified AlexNet," Stochastic Modeling & Applications, vol. 26, no. 3, pp. 1-10, Jan.-Jun. 2022.

[11] D. P. Yadav and S. Rathor, "Bone Fracture Detection and Classification using Deep Learning Approach," 2020 International Conference on Power Electronics & IoT Applications in Renewable Energy and its Control (PARC), GLA University, Mathura, UP, India, pp. 28-29, 2020.

[12] A. M. Tripathi, A. Upadhyay, A. Rajput, A. P. Singh, and B. Kumar, "Automatic detection of fracture in femur bones using image processing," in IEEE International Conference on Innovations in Information, Embedded and Communication Systems (ICIIECS), 2017, pp. 1-5.

[13] H. Y. Chai, K. L. Wee, T. T. Swee, S. H. Salleh, A. K. Ariff, and K. Kamarulafizam, "Gray-Level Co-occurrence Matrix Bone Fracture Detection," American Journal of Applied Sciences, vol. 8, pp. 26-32, 2011.

[14] Y. Ma and Y. Luo, "Bone Fracture Detection Through the Two-stage System of Crack-Sensitive Convolutional Neural Network," Journal Pre-proof, DOI: https://doi.org/10.1016/j.imu.2020.100452, 2020.

[15] J. E. Lee, Y. H. Seo, and D. W. Kim, "Convolutional Neural Network-Based Digital Image Watermarking Adaptive to the Resolution of Image and Watermark," Applied Sciences, vol. 10, no. 19, 6854, 2020, doi: 10.3390/app10196854.

[16] A. Tavakoli, Z. Honjani, and H. Sajedi, "Convolutional Neural Network-Based Image Watermarking using Discrete Wavelet Transform," arXiv:2210.06179v1 [eess.IV], 2022, pp. 1-10.

[17] I. de Pontes Oliveira, J. L. P. Medeiros, and V. F. de Sousa, "A Data Augmentation Methodology to Improve Age Estimation using Convolutional Neural Networks," IEEE, 2016.

[18] F. Hardalaç, F. Uysal, and O. Peker, "Fracture Detection in Wrist X-ray Images Using Deep Learning-Based Object Detection Models," MDPI Diagnostics, vol. 11, no. 1, pp. 1-12, 2021.

DOI: https://doi.org/10.54216/JCIM.160208
Received: January 30, 2025 Revised: March 23, 2025 Accepted: April 11, 2025

[19] S. S. Liew, M. Khalil-Hani, S. A. Radzi, and R. Bakhtieri, "Gender classification: a convolutional neural network approach," Turkish Journal of Electrical Engineering & Computer Sciences, vol. 24, pp. 1248 - 1264, 2016, doi: 10.3906/elk-1311-58.

[20] S. Bekhet, A. M. Alghamdi, and I. Taj-Eddin, "Gender recognition from unconstrained selfie images: a convolutional neural network approach," International Journal of Electrical and Computer Engineering (IJECE), vol. 12, no. 2, pp. 2066~2078, Apr. 2022, doi: 10.11591/ijece.v12i2.pp2066-2078.

[21] A. A. Abdulrahman and F. S. Tahir, "Distinguishing license plate numbers using discrete wavelet transform technology based deep learning," Indonesian Journal of Electrical Engineering and Computer Science, vol. 30, no. 3, pp. 1771~1776, Jun. 2023, doi: 10.11591/ijeecs.v30.i3.pp1771-1776.

[22] A. A. Abdulrahman et al., "Classification of food items in trash through images using a hybrid deep learning system," Eureka: Physics and Engineering, vol. 3, pp. 145-153, 2024.

[23] S. A. P. Rosyidi, N. I. Md. Yusoff, N. F. Nadia, and M. R. Mat Yazid, "Integrated time-frequency wavelet analysis and impulse response," Ain Shams Engineering Journal, vol. 12, pp. 367–380, 2021.

[24] M. Hatoum, J. F. Couchot, R. Couturier, and R. Darazi, "Using Deep Learning for Image Watermarking Attack," HAL Id: hal-03186561, 2021, pp. 116019.

[25] H. M. Muhi-Aldeen et al., "Technology of Secure Data Exchange in the IoT System," CEUR Workshop Proc., vol. 3200, pp. 115–121, 2021.

[26] A. R. Alshahrani and M. A. Alghamdi, "Real-time object detection for autonomous vehicles using deep learning techniques," Journal of Real-Time Image Processing, vol. 20, no. 1, pp. 123–134, 2023.

[27] J. K. Smith, A. M. Jones, and L. T. Green, "An efficient deep learning framework for medical image analysis," Journal of Medical Imaging and Health Informatics, vol. 14, no. 2, pp. 345–356, 2022.

[28] F. S. Tahir, A. A. Abdulrahman, and Z. H. Thanon, "Novel face detection algorithm with a mask on neural network training," International Journal of Nonlinear Analysis and Applications, vol. 13, no. 1, pp. 209–215, 2022, doi: http://dx.doi.org/10.22075/ijnaa.2022.547.

[29] M. A. Mustafa et al., "New algorithm based on deep learning for number recognition," International Journal of Mathematics and Computer Science, vol. 18, no. 3, pp. 429–438, 2023.

[30] H. M. Muhi-Aldeen et al., "Technology of Secure Data Exchange in the IoT System," CEUR Workshop Proc., vol. 3200, pp. 115–121, 2021.

DOI: https://doi.org/10.54216/JCIM.160208
Received: January 30, 2025 Revised: March 23, 2025 Accepted: April 11, 2025